Materials Science and Engineering A368 (2004) 280–285

www.elsevier.com/locate/msea

# The effect of strain path on the mechanical behavior and dislocation arrangements in the hot working of copper

P. Pinheiro [a], W.A. Monteiro [b], R. Barbosa [c], P.R. Cetlin [c,*]

[a] *Department of Mechanics, Federal Center of Technological Education of Minas Gerais, Belo Horizonte, Brazil*
[b] *Institute for Research on Nuclear Energy, São Paulo, SP, Brazil*
[c] *Department of Metallurgical and Materials Engineering, Federal University of Minas Gerais, Rua Espírito Santo 35-s206-Centro, 30.160-030, Minas Gerais, Belo Horizonte, Brazil*

Received 13 June 2003; received in revised form 3 November 2003

**Abstract**

Hot monotonic torsion of copper at 673 K led to a stress–strain curve displaying a peak and steady state stress typically connected to dynamic recrystallization (DRX). Cyclic deformation suppressed DRX, and restoration was dominated by Dynamic Recovery (DRV). Successive straining cycles involved the breakdown and restructuring of dislocation arrangements typical of DRV, causing a decrease in accumulated internal energy. These phenomena are similar to those caused by strain path changes under cold working conditions.


*Keywords:* Strain path; Copper; Hot working; Mechanical properties; Dislocation arrangements

## 1. Introduction

The ability of metals to be shaped by cold and hot plastic deformation (“cold or hot forming”) is one of their most important characteristics. Forming leads not only to shape changes but also to an increase in the strength of the material (“work hardening”), which depends on the material and the process variables (geometry, strain, strain rate, temperature and strain path). The effects of strain, strain rate and temperature have received wide attention in the literature, but analyses regarding the strain path have been less frequent, except for sheet metal forming [1–4]. There is an increasing interest on the strain path effects on hot working [5–9], because they influence the final microstructures and properties of the materials, as well as the required forming loads. In addition, changes in strain path profoundly alter the shape of the stress–strain curves of metals. The corresponding constitutive equations should reflect this, since they influence all the analytical and numerical approaches to metal forming problems.

Davenport [6] distinguishes between two types of strain paths—strain reversal (considering small strains and large strains separately) and other paths, such as sequentially orthogonal normal strains and combinations of normal and shear strains. Strain reversal is of technological importance in flat rolling, where reversed shears occur along the rolling gap. These are superimposed on an overall compression strain, and vary along the thickness of the rolled material. The rolling of long products involves an additional aspect, which is the use of successive deformation passes at 90° or 45° to each other. This component of straining is similar to pure multi-axial deformation (not superimposed on overall compression), which, similarly to cyclic straining in tension/compression [10], causes lower hardening than an equivalent monotonic strain [11–13]. The deformation in the cross section of long products is much more heterogeneous than in flat products [14], leading to increased levels of complexity in the analysis of this problem.

Industrial rolling of both flat and long products may involve a large number of passes (as much as 20) with varying time intervals between them [15]. There are some analyses covering the effect of strain path on the hot working of metals for such large number of passes, but most studies refer to

* Corresponding author. Tel.: +55-31-32381849; fax: +55-31-32381815.
*E-mail addresses:* ivetepinheiro@deii.cefetmg.br (P. Pinheiro), wamontei@net.ipen.br (W.A. Monteiro), rbarbosa@demet.ufmg.br (R. Barbosa), pcetlin@demet.ufmg.br (P.R. Cetlin).

0921-5093/$ – see front matter © 2003 Elsevier B.V. All rights reserved.
doi:10.1016/j.msea.2003.11.008

a few deformation steps. In general, the following aspects of processing have been covered: the shape of the stress–strain curves, the deformation mechanisms and the subsequent softening and final microstructures [7,8,12,16–18].

The present paper analyses the effects of strain path on the mechanical behavior and dislocation structures of metals, for the case of hot reversed shear and a large number of deformation passes. Copper was used as a model material because it has a FCC lattice and a relatively low stacking fault energy (SFE), leading to dynamic recrystallization (DRX) at working temperatures greater than 673 K. Copper displays no phase transformations upon cooling, and allows water quenching of samples for subsequent reliable studies of the microstructure. The 673–773 K processing temperatures are associated with very limited static restoration of the material during the time between deformation steps [16]. A clear separation of the effects of strain path and of static restoration on the experimental results is thus obtained [19]. The data for copper can be qualitatively extrapolated to the behavior of austenite, since these two materials have similar structural characteristics (FCC structure and relatively low SFE). Austenite has a greater technological significance than copper, but must be processed at a higher temperature (above approximately 1173 K) and does not allow simple microstructural studies through quenched samples, due to the inherent phase transformations.

## 2. Experimental procedures

Straining was carried out on a commercial purity copper (Sn: <0.10; P: 0.026; Pb: <0.01; Al: <0.03; Fe: 0.010; Mg: <0.001; Zn: 0.0035; Si: 0.024; Ni: <0.002; Cu: Bal.). The machined specimens (cylinders 6.35 mm in diameter and 15 mm in length) were annealed at 843 K for 5400 s in a vacuum of $1.01 \times 10^{-2}$ Pa and then cooled down to room temperature into the furnace.

Hot torsion tests were conducted in a servo-hydraulic, computer-controlled machine with a microprocessor controlled, tungsten lamp radiant furnace. The specimens were initially soaked at 843 K for 1800 s, cooled down to the testing temperature of 673 K at a rate of 1 K/s, and then thermally homogenized for 180 s. Tests were performed at a strain rate of $0.1\,s^{-1}$. The temperature was measured by a thermocouple in contact with the surface of the gauge length of the samples. Specimens were tested inside a quartz tube, through which flowed a protective argon atmosphere, in order to avoid sample oxidation. The measured values of torque ($\Gamma$), and angle of twisting ($\theta$), were converted to equivalent stress σ and strain ε [20,21], respectively, following Eqs. (1) and (2):

$$\sigma = \frac{3.3\sqrt{3\Gamma}}{2\pi R^3} \quad (1)$$

$$\varepsilon = \frac{\theta R}{\sqrt{3}L} \quad (2)$$

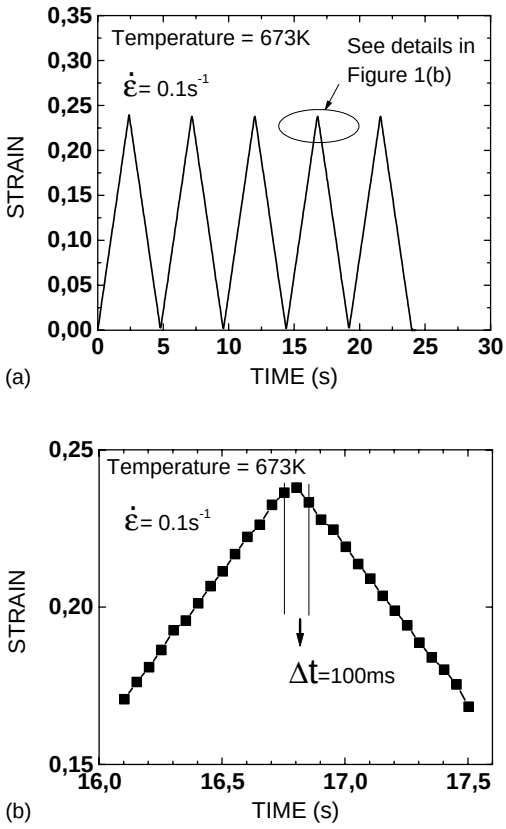


Fig. 1. (a) Experimental strain–time data for the initial cyclic torsion with a strain amplitude $\Delta\varepsilon = 0.24$ and a strain rate $0.1\,s^{-1}$, (b) details of the experimental data in the region of the strain peak in the 4th cycle.

where $L$ and $R$ are the gauge length and radius of the specimen, respectively.

Cyclic torsion involved programming the twist angle and speed of the torsion machine so that the desired strain amplitude (as per Eq. (2)) and strain rate would be obtained. Fig. 1(a) shows the evolution of strain for the present experiments, for a strain amplitude $\Delta\varepsilon = 0.24$. Fig. 1(b) displays the experimental details around the fourth strain cycle peak. The linear portions of this graph, before and after the peak, indicate a strict adherence to the programmed strain rate ($0.1\,s^{-1}$). It can also be seen that the strain went through a full reversal in a time interval $\Delta t = 100$ ms. The examination of other experimental data revealed that Δt never exceeded 200 ms. An investigation was performed in order to analyze the effect of these resting periods on the softening between passes. The analysis utilized the method of Petkovic et al. [22,23], which indicated that no significant static softening occurred up to a time interval of 200 ms for reversing the straining direction.

The microstructural observations after monotonic and cyclic tests were performed following quenching of the specimens, which involved water flooding the quartz tube containing the samples. There was a time lag of 0.8 s between the opening of the water valve and the beginning of

quenching. The furnace was turned off simultaneously with the introduction of water. The measured specimen cooling during this 0.8 s lag was below 1 K. Thus there was very little time during which the material was at high temperature and not being strained. $H_2O$ quenching cooled the sample surface from 673 to 473 K in about 0.5 s.

The observation of dislocation structures was performed using transmission electronic microscopy (TEM). Sections were taken close to the surface and parallel to the longitudinal axis of the torsion specimen. Small disks (3 mm diameter) were cut and subsequently carefully ground down to a thickness of approximately 100–160 μm. The disks were thinned at 278 K in a double jet electropolishing operation (80% ethanol and 20% nitric acid), using a Tenupol III (Struers) apparatus.

## 3. Results and discussion

Fig. 2(a) shows the experimental monotonic equivalent stress–strain curve (SS curve). Its shape indicates that dynamic recrystallization (DRX) occurs during the test, leading to a steady state stress after strains approximately larger than 1.25. An analysis of the work hardening rate–stress curve

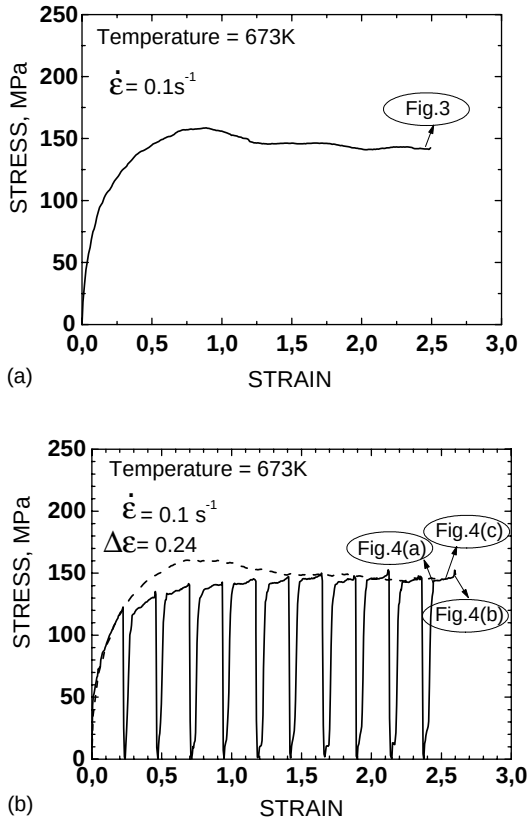


Fig. 2. (a) Equivalent stress–strain curve for the monotonic torsion testing, rotation in the counter-clockwise direction (+). (b) Cyclic SS curve for a strain amplitude $\Delta\varepsilon = 0.24$ over 11 cycles.

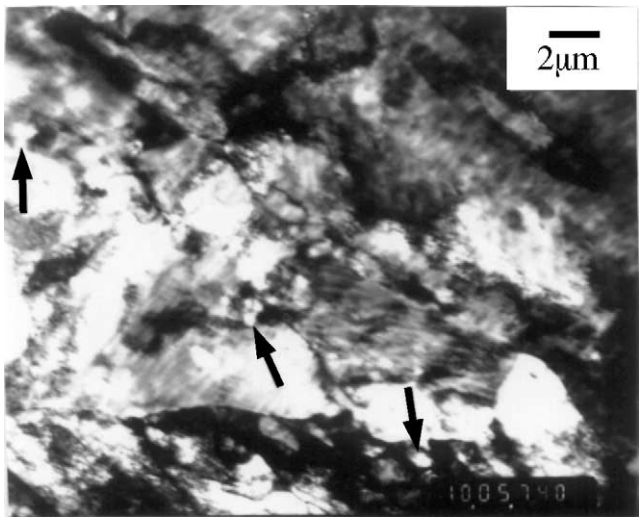


Fig. 3. TEM observation on longitudinal near surface sections after monotonic straining to $\varepsilon = 2.5$; dark areas correspond to heavily deformed grains; bright areas represent dynamically recrystallized grains; arrows indicate dynamically recrystallized grain nuclei.

[12], led to a peak stress $\sigma_p = 158.7$ MPa and a corresponding peak strain $\varepsilon_p = 0.89$. It is also possible to evaluate [12] the critical strain for the initiation of DRX and the respective value of the stress ($\varepsilon_c = 0.68$ and $\sigma_c = 152.7$ MPa).

Fig. 2(b) shows the experimental SS curve for the cyclic loading with a strain amplitude of $\Delta\varepsilon = 0.24$, where the stresses and strains are always taken as positive, and the strain per cycle is cumulative [18]. This allows a comparison with the SS curve for monotonic torsion (dashed line, Fig. 2(b). The curve for cyclic straining does not display a peak stress, suggesting that DRX is not occurring. The envelope for the cyclic SS curves in Fig 2(b) progressively approaches the same steady state stress ($\sigma_{ss}^{c}$) as that for the monotonic curve ($\sigma_{ss}$). It was previously shown [16] for copper deformed at 773 K, that cyclic and monotonic straining led to approximately the same steady state stress for ratios $\Delta\varepsilon/\varepsilon_p$ above unity. In the present case, at 673 K, such a situation was observed for a much lower ratio $\Delta\varepsilon/\varepsilon_p = 0.24/0.89 = 0.27$. This is probably connected to the lower levels of dynamic recovery (DRV) at 673 K, as compared to deformation at 773 K.

TEM analysis showed that monotonic torsion led initially to dislocation microbands, which are then divided by dislocation walls along their length, producing elongated sub-grains, similar to that in Akbari et al. [24]. Increased deformation led to the loss of these bands and to the appearance of new dynamically recrystallized grains (Fig. 3), which corresponds to a total strain of 2.5, as indicated in Fig. 2(a). Some grains are heavily deformed and display a dense substructure (dark areas), while other grains present almost no substructure (brighter areas), indicating that dynamic recrystallization had occurred. Additionally, the presence of some nuclei (arrows) was identified.

Fig. 4(a) and (b) show the dislocation structures in pure Cu at the end of the 10th cycle (counterclockwise rotation, total strain of $\varepsilon = 2.4$) and at the end of the 11th cycle (clockwise rotation, $\varepsilon = 2.64$), respectively, as indicated in Fig. 2(b). The dislocation arrangements present in the substructure at the end of each deformation cycle differ strongly from that observed for the monotonic tests (see Fig. 3), for approximately the same total strains. Profuse dislocation microbands are now observed, displaying some walls along their lengths. No dynamically recrystallized grains or nuclei can be seen. The features shown in Fig. 4(a) and (b) are similar to those observed in the initial stages of monotonic straining, as well as those commonly associated with dynamic recovery in the cold working of FCC metals [25]. DRV is the prevailing restoration mechanism during the cyclic working of copper at 673 K, even to quite large deformations. Cyclic straining seems to decrease the accumulation of internal energy connected to plastic working, in comparison to monotonic straining. As a result, DRX is not triggered and restoration is dominated by DRV. It is conceivable that, as the strain per cycle increases towards a higher fraction of the critical strain for the beginning of DRX or of the peak strain (estimated to be $\varepsilon_c = 0.68$ and $\varepsilon_p = 0.89$, respectively, in the present case), one will end up with increasing degrees of DRX at the end of each successive cycle.

In order to allow further insight into the prevailing deformation mechanisms during cyclic torsion, a TEM observation was performed at a point in between the situations in Fig. 4(a) and (b). This was taken at a total strain of 2.5, midway between the end of the 10th cycle (counterclockwise rotation, total strain of $\varepsilon = 2.4$) and the end of 11th cycle (clockwise rotation, total strain of $\varepsilon = 2.64$), as indicated in Fig. 2(b), and a typical structure is displayed in Fig. 4(c). The dislocation microband structure has disintegrated: many of the microband boundaries cannot be clearly observed, and the overall dislocation structure is much more disperse than in the starting microband structure shown in Fig. 4(a). On the other hand, a diffuse "blocky" cell structure is delineated, which corresponds to the remnants of the old structure and to a new microband structure being formed at 90° with the old one. Further deformation leads to the elimination of the previous microbands and to the full development of a new set of microbands, as shown in Fig. 4(b). One concludes that the lack of sufficient stored energy for triggering DRX is the result of the successive disintegration and build-up of dislocation structures, during strain reversal.

The present results show that the restoration mechanisms and resulting dislocation structures in monotonic straining are very different from those prevailing in cyclic deformation. The former is dominated by DRX, whereas the latter is controlled by DRV through the cyclic disintegration and build up of dislocation microbands. It is surprising that two such different microstructures, which are certainly associated with differing internal stress patterns, can lead to ba-

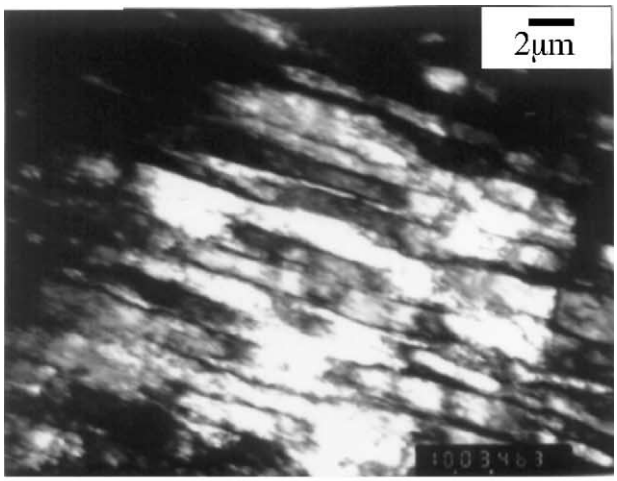


(a)

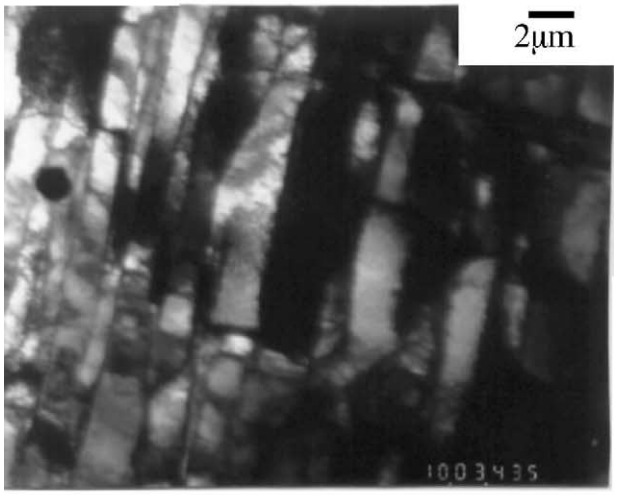


(b)

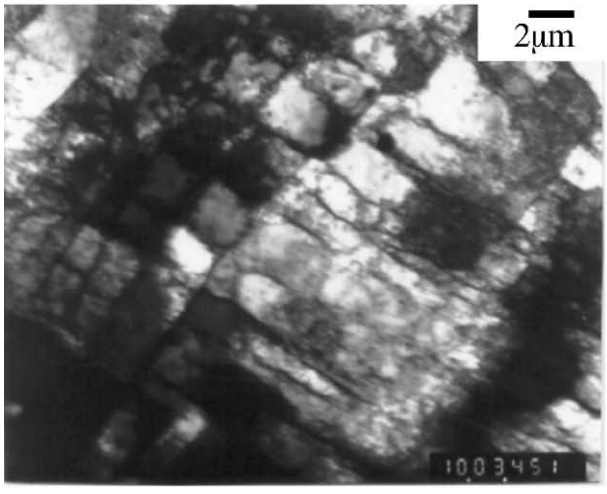


(c)

Fig. 4. TEM observation on longitudinal near surface sections after (a) cyclic straining to $\varepsilon = 2.4$ (end of 10th cycle, counterclockwise rotation); (b) cyclic straining to $\varepsilon = 2.64$ (end of the 11th cycle, clockwise rotation); (c) cyclic straining to $\varepsilon = 2.5$ (midway between the 10th and the 11th cycle applied as a clockwise rotation).

sically the same macroscopic steady state stress levels. It should be remembered, however, that cyclic straining with strain amplitudes lower than those presently employed, lead to decreased levels of work hardening and to values of the steady state stress substantially below those for monotonic straining [8,16,18].

The restructuring of dislocation structures caused by strain path changes has already been reported for the case of cold working. Huang [26] describes extensive dislocation restructuring caused by a decrease in plastic deformation amplitude (from 0.003 to 0.001) during low cycle fatigue. Lopes et al. [19] and Bate [27] indicate the presence of a cell restructuring mechanism in the cold working of an AA1050 aluminum alloy, which bears striking similarities to the present experimental results for the hot working of copper. Fernandes [28] observed dislocation restructuring in copper deformed in tension followed by shearing at room temperature. Strauwen and Aernoudt [29] also reported such restructuring during the compression of initially cold drawn low carbon steel bars. The phenomena described in the present paper are thus in line with observations already developed for cold working. On the other hand, the possible presence of DRX in hot working introduces a new dimension to the problem, since it can be completely eliminated by the decreased driving force for DRX associated with cyclic straining.

Another interesting aspect of the present work is that, for the initial five cycles of reversed straining, the shapes of the successive SS curves resemble those recently described by Bartolomé et al. [30]. There is an initial fall in the yield stress of each cycle in relation to the monotonic curve, which is attributed to a Bauschinger effect. A stress “plateau” follows, during which some type of dislocation structure rearrangement would occur, exactly as described in the present paper. On the other hand, cyclic straining into the steady state regime does not display such a Bauschinger effect in each cycle, whose initial part is already quite close to the monotonic stress–strain curve. This means that the directional effects of the prevailing dislocation arrangements become non-existent or ineffective, after a sufficient number of cycles.

## 4. Summary

(1) Dynamic recrystallization was observed in the monotonic torsion of copper at 673 K under a strain rate $\dot{\varepsilon} = 0.1\,s^{-1}$, promoting extensive grain refinement.
(2) The cyclic torsion stress–strain curve of copper at 673 K, under a strain rate $\dot{\varepsilon} = 0.1\,s^{-1}$ and a strain amplitude $\Delta\varepsilon = 0.24$ did not display the characteristic DRX peak. TEM evidence indicated the absence of DRX even after a large amount of straining. The sole observed restoration mechanism was dynamic recovery.
(3) Cyclic torsion of copper under the above-mentioned experimental conditions involved the successive disintegration and build-up of dislocation microbands. The accumulated strain energy was not sufficient to trigger DRX.
(4) The dislocation restructuring phenomena observed in the present research are similar to those reported for strain path changes under cold working. Such restructuring caused enhanced levels of DRV, eliminating the DRX observed under monotonic straining.

## Acknowledgements

The authors are grateful for the financial support of the PRONEX (Programa de Núcleos de Excelência) from the Ministério de Ciência e Tecnologia, and of the CNPQ (Conselho Nacional de Desenvolvimento Científico e Tecnológico). CDTN/CNEN (Centro de Desenvolvimento de Tecnologia Nuclear/Comissão Nacional de Energia Nuclear), kindly vacuum annealed the specimens.

## References

[1] A.K. Ghosh, W.A. Backofen, Metall. Trans. 4 (1973) 1113.
[2] D.J. Loyd, H. Sang, Metall. Trans. A 10 (1979) 1767.
[3] R.H. Wagoner, Metall. Trans. A 133 (1982) 1491.
[4] J.V. Fernandes, M.F. Vieira, Metall. Trans. A 28 (1997) 1169.
[5] S.B. Davenport, R.L. Higginson, C.M. Sellars, Philos. Trans R. Soc. London A 357 (1999) 1645.
[6] S.B. Davenport, R.L. Higginson, J. Mater. Process. Technol. 98 (2000) 267.
[7] E. Lindh, B. Hutchinson, S. Ueyama, Scripta Metall. 29 (1993) 347.
[8] I.P. Pinheiro, R. Barbosa, P.R. Cetlin, in: Proceedings of the Thermomechanical Processing of Steel J.J. Jonas Symposium, Met. Soc., Ottawa, 2000, p. 221.
[9] R.L. Higginson, C.M. Sellars, Mater. Sci. Eng. A 338 (2002) 323.
[10] L.F. Coffin, J.F. Tavernelli, Trans. Metall. Soc. AIME 215 (1959) 794.
[11] P.E. Armstrong, J.E. Hockett, J. Mech. Phys. Solids 30 (1982) 37.
[12] X.J. Zhang, P.D. Hodgson, P.F. Thomson, in: Proceedings of the Australiasia Pacific Forum on Intelligent Processing and Manufacturing of Materials–IPPMM, Brisbane, Australia, National Library of Australia, Brisbane, 1997, p. 941.
[13] X.J. Zhang, P.F. Thomson, P.D. Hodgson, in: Proceedings of the Conference on Thermomechanical Processing of Steels and Other Materials—THERMEC, Pennsylvania, TMS, Warrendale, PA, 1997, p. 1705.
[14] S. Choi, Y. Lee, P.D. Hodgson, J. Mater. Process. Technol. 124 (2002) 329.
[15] P.R. Cetlin, S. Yue, J.J. Jonas, ISIJ Int. 33 (1993) 488.
[16] I.P. Pinheiro, R. Barbosa, P.R. Cetlin, Scripta Mater. 44 (2001) 187.
[17] Q. Zhu, C.M. Sellars, in: Proceedings of the Conference on Thermomechanical Processing in Theory Modelling and Practice (TMP), Stockholm, Sweden, September 4–6, 1996, ASM, Materials Park, OH, 2000, p. 193.
[18] I.P. Pinheiro, R. Barbosa, P.R. Cetlin, Scripta Mater. 38 (1998) 53.
[19] A.B. Lopes, F. Barlat, J.J. Gracio, J.F. Ferreira Duarte, E.F. Rauch, Int. J. Plast. 19 (2003) 1.
[20] T.M. Maccagno, J.J. Jonas, S. Yue, B.J. McCrady, R. Slobodian, L. Deeks, ISIJ Int. 34 (1994) 917.
[21] T.M. Maccagno, J.J. Jonas, ISIJ Int. 34 (1994) 607.
[22] R.A. Petkovic, M.J. Luton, J.J. Jonas, Can. Metall. Quarterly 14 (1975) 137.

[23] R.A. Petkovic, M.J. Luton, J.J. Jonas, Acta Metall. 27 (1979) 1633.
[24] G.H. Akbari, C.M. Sellars, J.A. Whiteman, Acta Mater. 45 (1997) 5047.
[25] D. Kuhlman-Wilsdorf, Acta Mater. 47 (1999) 1697.
[26] H.L. Huang, Mater. Sci. Eng. 342 (2003) 38.
[27] P.S. Bate, Metall. Trans. A 24 (1993) 2679.
[28] J.V. Fernandes, J.J. Gracio, J. H. Schmitt, Scripta Metall. Mater. 28 (1993) 1355.
[29] Y. Strauwen, E. Aernoudt, Acta. Metall. 35 (1986) 1029.
[30] R. Bartolomé, D. Jorge-Badiola, J.I. Astiazarán, I. Gutiérrez, Mater. Sci. Eng. A 344 (2003) 340.